Electronic Supplementary Material (ESI) for Catalysis Science & Technology.

Supporting information

Brönsted Acid-Enhanced CoMoS Catalyst for Hydrodeoxygenation Reaction

Yijin Zhang[a], Tangkang Liu[a], Hongyan Jia[b,*], Qineng Xia[b], Xinlin Hong[a], Guoliang Liu[a,*]

[a] College of Chemistry and Molecular Sciences, Wuhan University, Wuhan 430072, PR China.

[b] College of Biological, Chemical Science and Engineering, Jiaxing University, Jiaxing 314001, PR China.

* The corresponding authors. E-mail address: liugl@whu.edu.cn; jiahy@zjxu.edu.cn

Experimental Section

Chemicals and Materials

Ammonium molybdate tetrahydrate [$(NH_4)_6Mo_7O_{24}\cdot 4H_2O$], cobalt nitrate hexahydrate ($Co(NO_3)_2\cdot 6H_2O$), thiourea [$CS(NH_2)_2$], absolute ethanol, hydrochloric acid, decahydronaphthalene, zirconium oxide (ZrO_2), phosphotungstic acid hydrate ($H_3O_{40}PW_{12}\cdot xH_2O$) and phosphomolybdic acid hydrate ($H_3Mo_{12}O_{40}P\cdot xH_2O$) were purchased from Sinopharm Chemical Reagent Co., Ltd. *p*-Cresol, silicotungstic acid hydrate ($H_4[Si(W_3O_{10})_4]\cdot xH_2O$) and ceria were purchased from Shanghai Aladdin Biochemical Technology Co., Ltd. *γ*-Aluminumoxide was purchased from Innochem Co., Ltd. Silicon oxide was purchased from Tianjin Nankai Chemical Plant. Titanium oxide was purchased from Shanghai D&B Biological Science and Technology Co., Ltd. n-Octane was purchased from Jiangsu Qiangsheng Functional Chemical Co., Ltd. All the reagents used in the experiment were of analytical grade and used without further purification.

Synthesis of pristine MoS_2

Ammonium molybdate tetrahydrate (0.275 mmol) and thiourea (18 mmol) were dissolved in 50 mL distilled water. Hydrochloric acid (35 wt%) was dropped into the solution until the pH<0.9. After stringing for 0.5 h, the solution was then transferred into a 100 mL Teflon-lined stainless autoclave and heated at 200 ^oC for 24 hours. The resulting black precipitate was separated by centrifugation and washed three times with water and ethanol. Subsequently, the MoS_2 was obtained by vacuum dried at 60 ^oC for 8 hours.

Synthesis of pristine CoMoS

100 mg MoS_2 was dispersed into 36 mL ethanol, and then 4 mL cobalt nitrate solution (0.094 M) was added to this dispersion solution. The mixed solution was then transferred into a Teflon-lined stainless autoclave and treated at 150 ^oC for 3 hours. The precipitate was separated by centrifugation, washed with water and absolute ethanol, and dried under vacuum at 60 ^oC. Then, the powder was reduced to 15 mL decalin at 300 ^oC, 3 MPa for 3 hours in a sealed autoclave. At last, the desired product was separated and washed with water and absolute ethanol three times and dried at 60 ^oC in a vacuum oven.

Synthesis of $NbOPO_4$

$NbOPO_4$ used in this work was synthesized by a hydrothermal method according to the literature [1]. Typically, 1.98 g $(NH_4)_2HPO_4$ and 2.70 g concentrated phosphoric acid (98 %) were dissolved in 30 mL deionized water. Then, 30 mL niobium tartrate (0.5 M) was added to the above solution. Afterward, the mixed solution was dropped into the aqueous solution previously prepared by dissolving 1.5 g cetyltrimethyl ammonium bromide (CTAB) in 20 mL of deionized water at 35 °C. After stirring for an additional 1 h, the obtained suspension was aged for 24 h at 160 °C. After cooling down, the solid was filtered, washed with deionized water and ethanol, then dried at 80 °C overnight and calcined at 500 °C for 5 h in the air to obtain $NbOPO_4$ material.

Synthesis of CoMoS/X

The CoMoS-NbP was fabricated by physical mixing a certain percentage (set $CoMoS/NbOPO_4$=5:0, 9:1, 4:1, and 3:2 in the weight ratio) of CoMoS with $NbOPO_4$ by grinding. The CoMoS/X was offered by mixing Co-MoS_2 with other support (X=$H_4[Si(W_3O_{10})_4]\cdot xH_2O$, $H_3O_{40}PW_{12}.xH_2O$, $H_3[P(Mo_3O_{10})_4]$, SiO_2, Al_2O_3, ZrO_2, CeO_2, and TiO_2, and CoMoS/X=4/1 in the weight ratio) by the same method.

Characterization

X-ray diffraction (XRD) patterns were recorded on a Rigaku Miniflex600 powder diffractometer with a Cu Kα radiation (a generator operated at 40 kV and 15 mA) to confirm the crystal structure of samples. Scanning electron microscopy (SEM, FEI Verios460) and transmission electron microscopy (TEM, FEI Tecnai G2 F20) images were captured, to demonstrate the morphologies of catalysts. X-ray photoelectron spectroscopy (XPS) spectra were recorded on a Thermo Scientific K-Alpha+ X-ray Photoelectron Spectrometer with a monochromatic Al Kα source with an energy of 1486.6 eV and operating power of 225 W (15 kV, 15 mA). Raman was carried out on Thermo Fischer DXR, with an excitation wavelength of 532 nm.

The H_2 temperature-programmed reduction (H_2-TPR) experiment was conducted using a Micromeritics Autochem 2920 equipped with a thermal conductivity detector (TCD). Typically, 30 mg of sample was treated at 150 °C for 1 h under high-purity Ar flow (30 mL min^{-1}). After cooling down to ambient temperature, the gas was changed to 5 vol% of H_2/Ar (30 mL min^{-1}). Subsequently,

the sample temperature was ramped from ambient temperature to 800 °C at a rate of 10 K min^{-1}. NH_3-TPD measurements were performed as the same. The catalyst was pretreated at 150 °C for 1 h before saturation with NH_3 at 100 °C and heating to 800 °C at 10 °C min^{-1}.

Diffuse-reflectance infrared Fourier transform spectroscopy (DRIFTS) spectra of pyridine adsorption were obtained on a Bruker VERTEX 70 (equipped with an MCT detector). The resolution and scan number were set at 4 cm^{-1} and 64, respectively. Typically, the catalyst was pre-treated at 230 °C for 1 h under 10 vol% H_2/Ar flow (30 mL·min^{-1}) and then evacuated before being cooled down to 30 °C under high purity Ar flow. The background spectra were collected at 200, 150, 100, and 30 °C. After that, the pyridine vapor was purged into the Ar flow. After adsorbing pyridine for 30 min, the gas was switched to high purity Ar flow (30 mL min^{-1}). In the meantime, the time-resolved DRIFTS spectra were collected at each temperature.

Catalytic testing

Hydrodeoxygenation (HDO) reaction of *p*-cresol was carried out in a 60 mL sealed high-pressure autoclave with a glass liner. Before each test, 50 mg of catalyst was dispersed into 15 mL of decalin (solvent) and then 420 mg of *p*-cresol and 420 mg of octane (internal standard) were added to the above solution. The autoclave was purged with hydrogen gas several times to evacuate the air, and then pressurized to 3 MPa and heated to 230 °C. After the reaction, a small amount of liquid sample was collected and analyzed by gas chromatography equipped with an FID detector. All experiments were repeated at least three times to ensure the reproducibility of the data, and the carbon balance was >95 %. After the reaction, a small amount of supernatant has been taken for quantitative testing. Then, replenish the reactant to a certain amount and start the second run. Subsequent experiments are repeated in this way. The reaction rate constant of HDO of *p*-cresol was calculated by following a pseudo-first-order reaction as below:

$$\ln(1-x) = -kC_{CoMoS}t \quad (1)$$

in which k is the pseudo-first-order rate constant (mL·mg^{-1}·h^{-1}), x is the conversion of *p*-cresol, C_{CoMoS} is the mass concentration of CoMoS under the reaction system and t is the reaction time (h).

Screening of mixing methods

After pre-reduction in 300 °C, the reduced CoMoS was mixed with $NbOPO_4$ in four ways (Figure S1a), and the mass ratio of CoMoS to $NbOPO_4$ keeps constant at 3:2 in all cases. The CoMoS and $NbOPO_4$ were mixed by grind in method **a**, and dispersed in ethanol at 150 °C by solvothermal in method **b**. In method **c**, they were mixed by calcinating at 300 °C. In method **d**, the $NbOPO_4$ was used as a support to load MoS_2 and Co species. The HDO reaction of *p*-cresol was performed in a batch-mode autoclave at 230 °C and 3.0 MPa for 3 h. As the results are shown in Figure S1, powder mixing in the method **a** presents higher activity and toluene selectivity than the others.

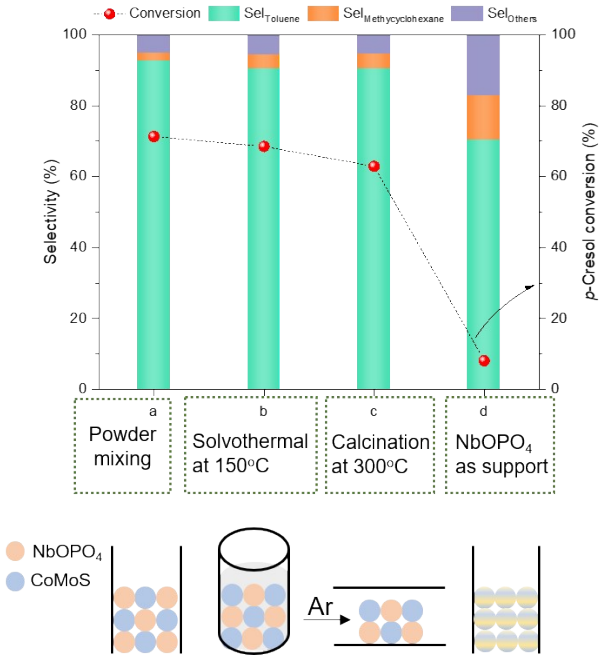

Figure S1. Catalytic performance of the conversion and selectivity of four different methods of mixing of CoMoS with $NbPOPO_4$.

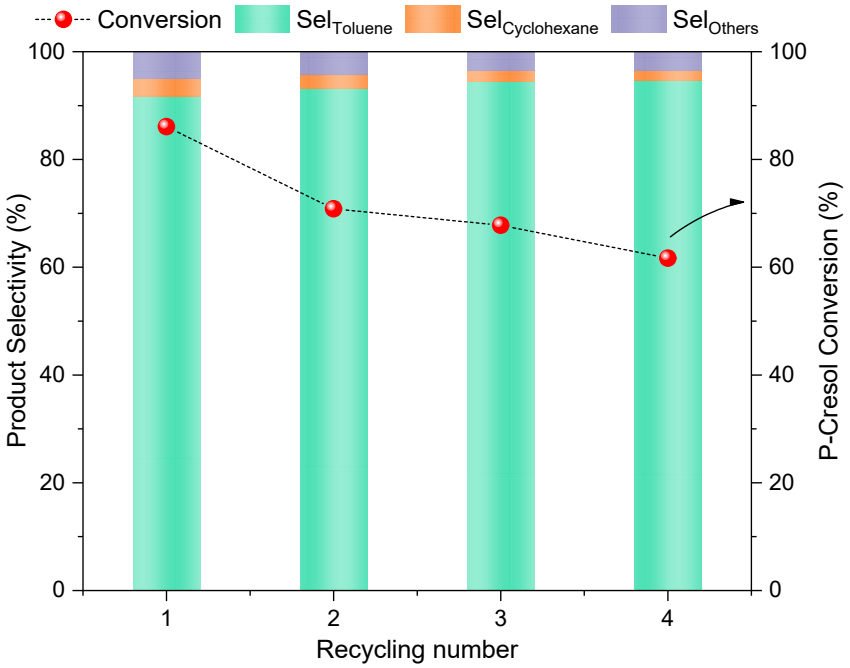

Figure S2. Catalytic stability test of CoMoS/NbP-4 in the HDO of p-cresol.

Table S1. the BET surface area of the CoMoS and $NbOPO_4$ sample.

Sample	Surface area ($m^2 \cdot g^{-1}$)
CoMoS	45.1
$NbOPO_4$	207.1

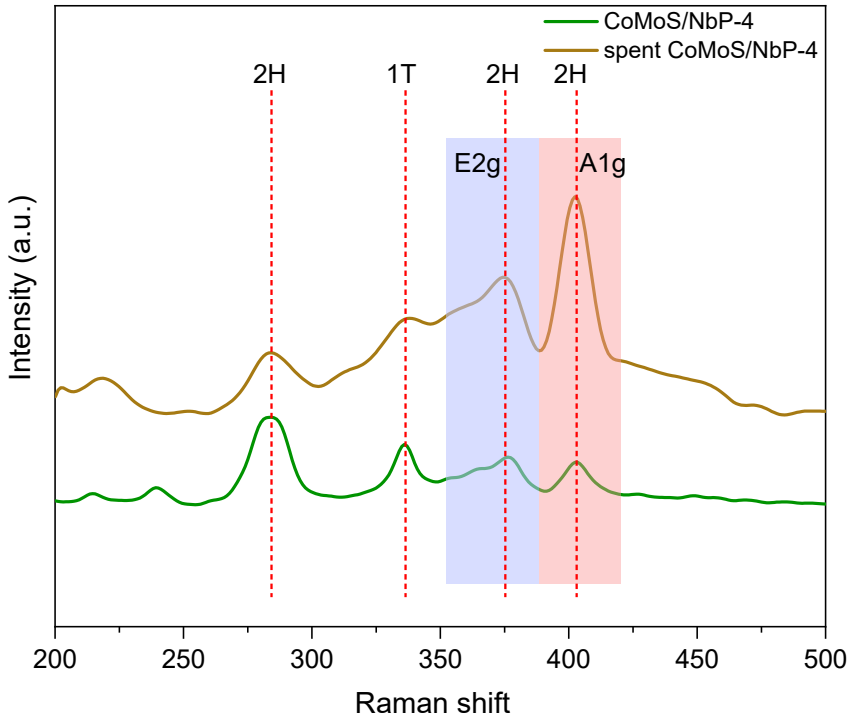

Figure S3. Raman spectra of the fresh and spent CoMoS/NbP-4 samples.

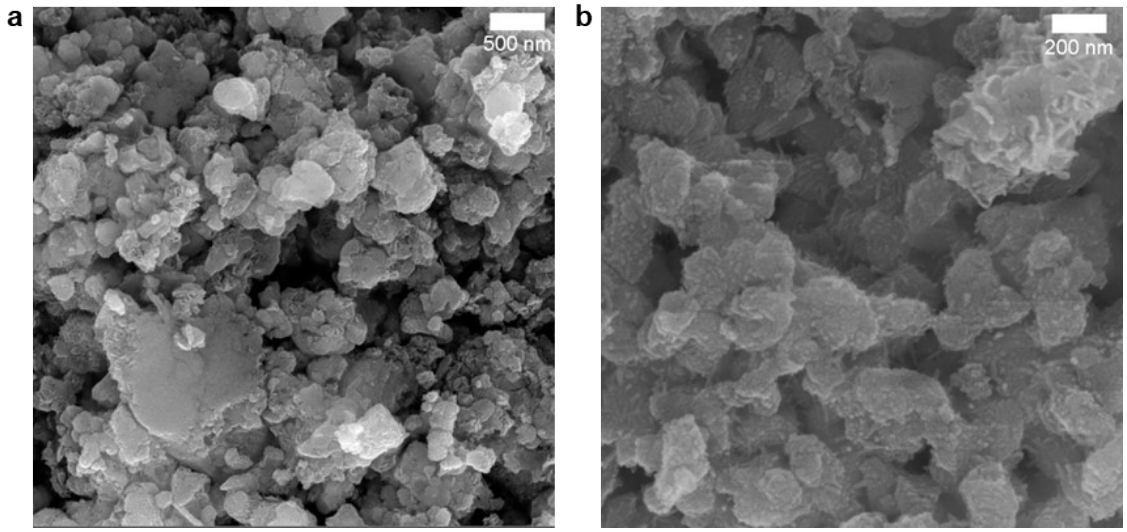

Figure S4. SEM images of the representative CoMoS/NbP-4 sample before reaction

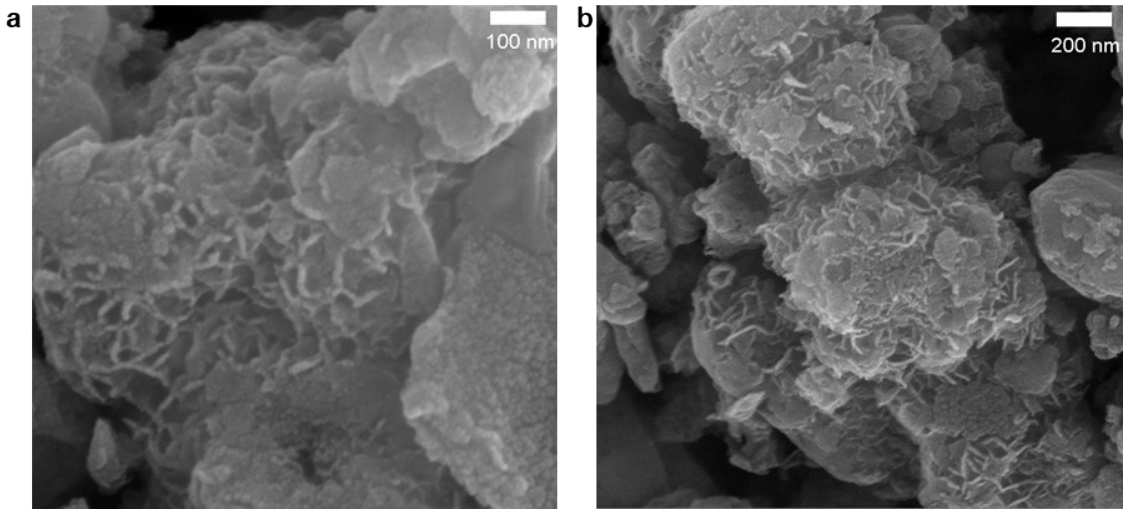

Figure S5. SEM images of the CoMoS/NbP-4 sample after the reaction.

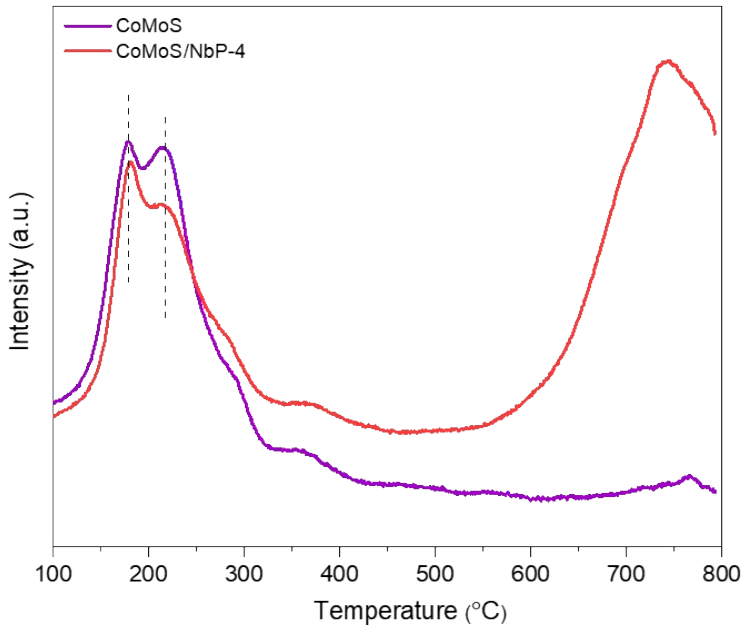

Figure S6. H_2-TPR spectra of the CoMoS/NbP-4 sample before and after mixing.

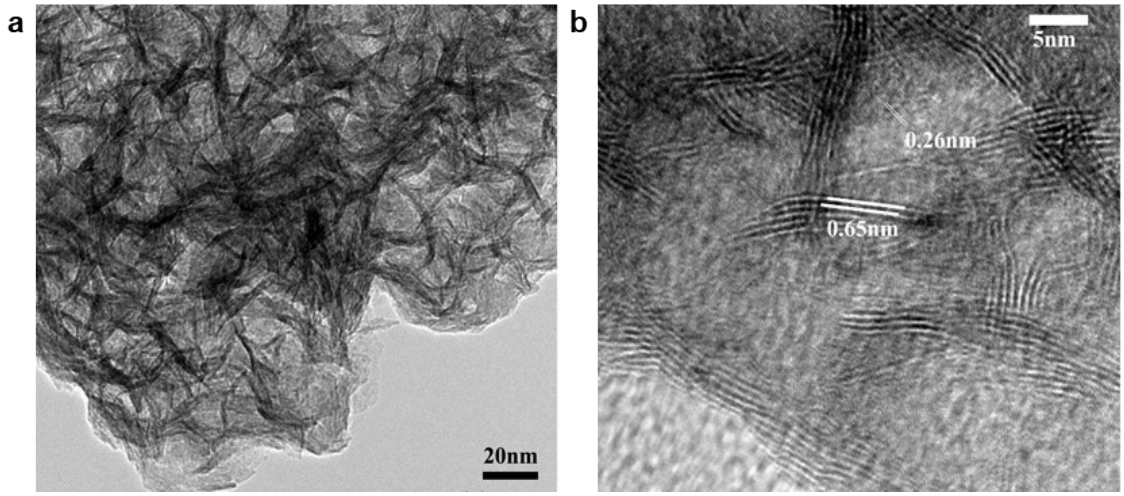

Figure S7. TEM and HRTEM images of the CoMoS/NbP-4 sample.

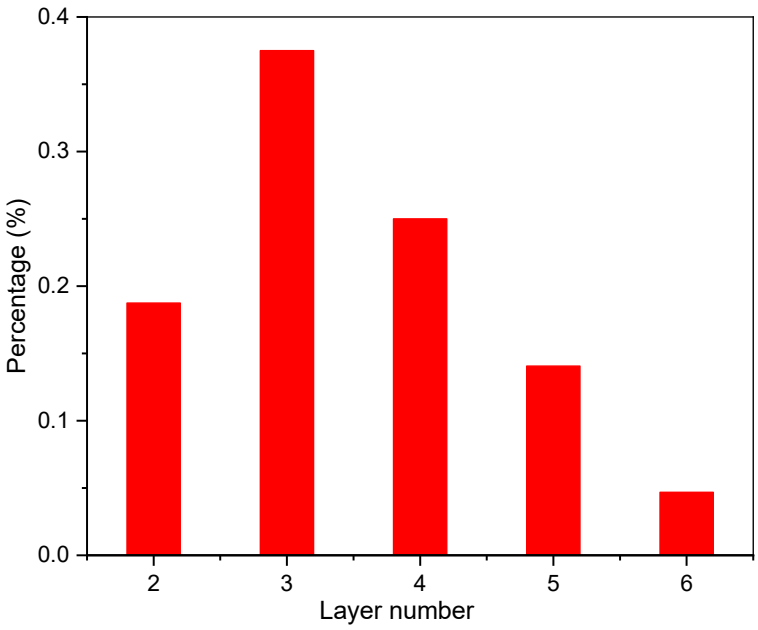

Figure S8. The histogram of layer distribution from HRTEM images (see Figure 2 and S6) of the CoMoS/NbP-4 sample.

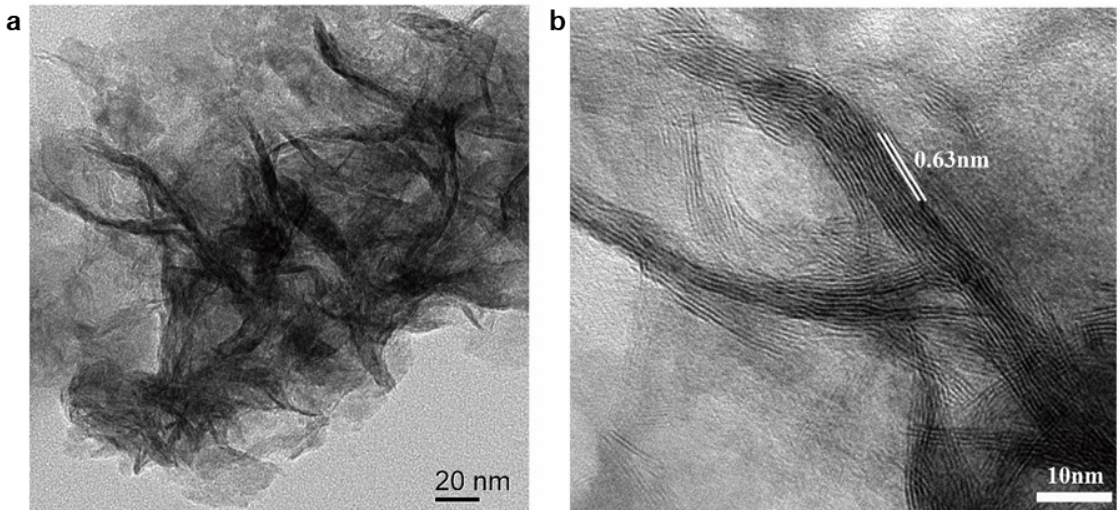

Figure S9. TEM and HRTEM images of the spent CoMoS/NbP-4 sample.

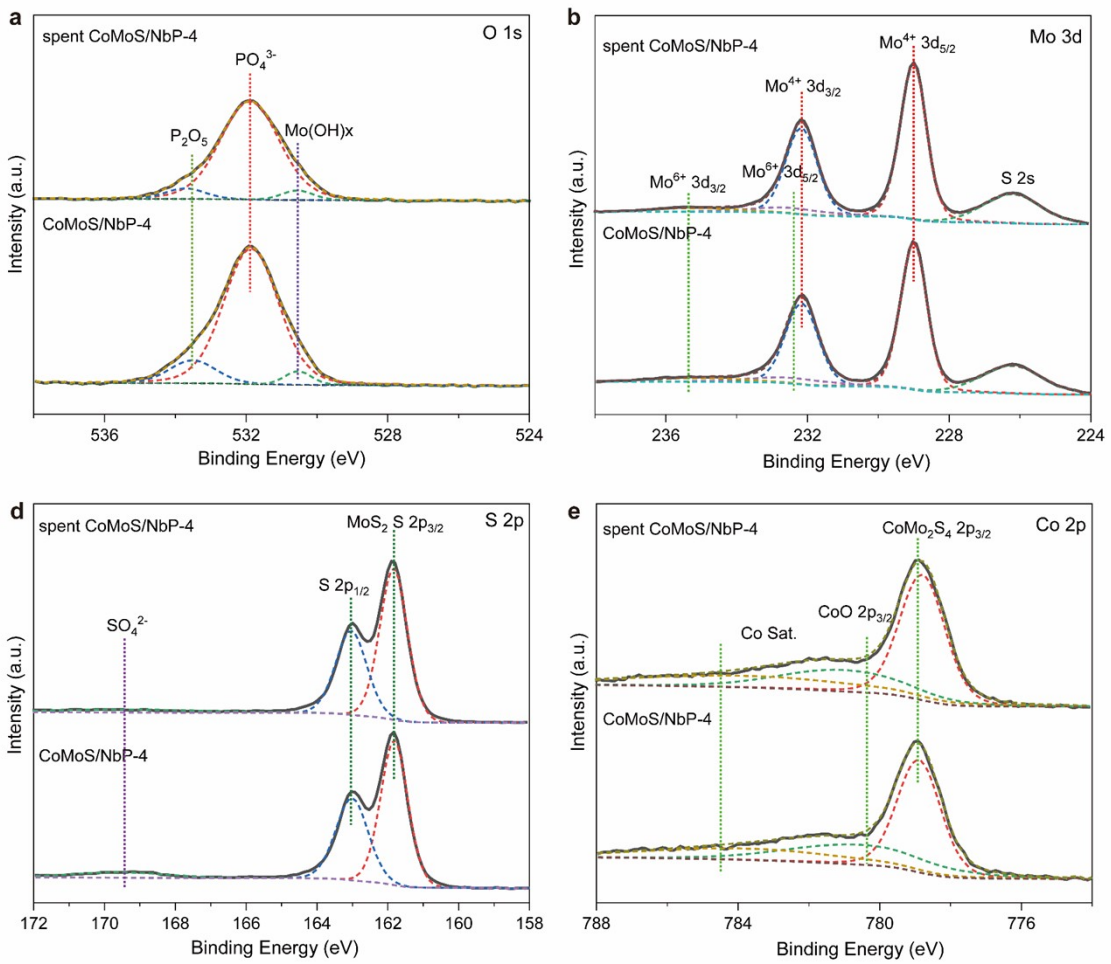

Figure S10. Deconvolution of the (a) O 1p, (b) Mo 3d (c) S 2p and (d) Co 2p regions (in XPS data) of the CoMoS/NbP-4 catalysts before and after the reaction.

The high-resolution XPS was also taken to specify the structure on the surface of the composite catalysts before and after the reaction in Figure S8. In the O 1s XPS spectra (Figure S9a), the peak at 532 eV and 533.5 eV is assigned to P_2O_5 and PO_4^{3-} which belong to $NbOPO_4$ [2]. The large part of PO_4^{3-} may indicate that large Brönsted acid sites exist on the composite catalyst. After the HDO reaction, the peaks of P_2O_5 and PO_4^{3-} do not change, indicating the chemical environment of $NbOPO_4$ is the same as before [2,3]. And the peak at 530.6 eV belongs to the $Mo(OH)_x$ on the surface of the MoS_2 [4]. In the Mo 3d XPS spectra (Figure S9b), the peak at 232.1 and 229.0 eV attributed to Mo^{4+} $3d_{3/2}$ and $3d_{5/2}$ spectra of MoS_2 [5~7]. And the doublet peak at higher binding energy (235.4 and 232.4 eV) is assigned to Mo^{6+} of the MoO_xS_y phase, suggesting the partial oxidation of the catalysts [7~9]. The S 2p spectra of the fresh and spent CoMoS/NbP-4, as shown in Figure S9c, the peaks at 163.0 eV, 161.8 eV are assigned to MoS_2 [10,11]. Figure S9d shows the

deconvolution of the Co 2p spectra. The peak at 778.9 eV is attributed to the typical Co-Mo-S phase on the surface of catalysts [12]. The peak at 780.4 eV is attributed to CoO_x species, the peak accompanied to which at 784.5 eV is a satellite peak of Co species [6].

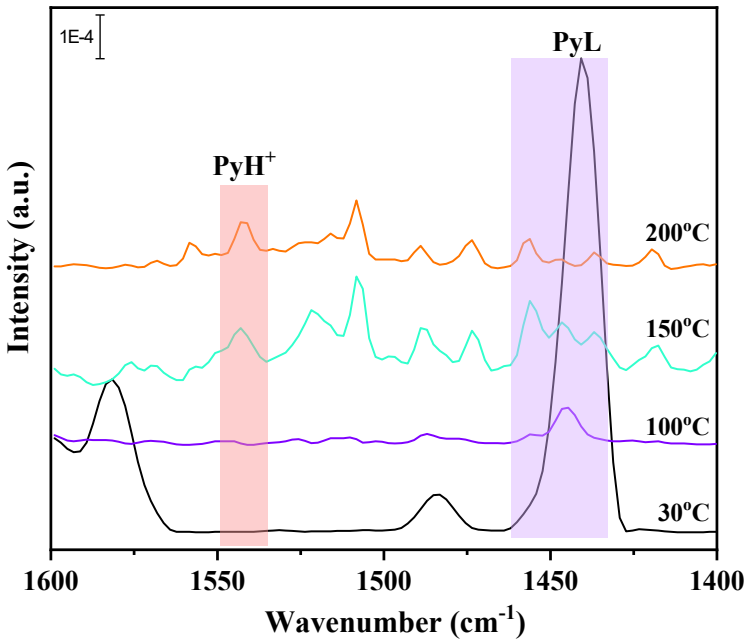

Figure S11. Pyridine-IR spectra of the CoMoS sample.

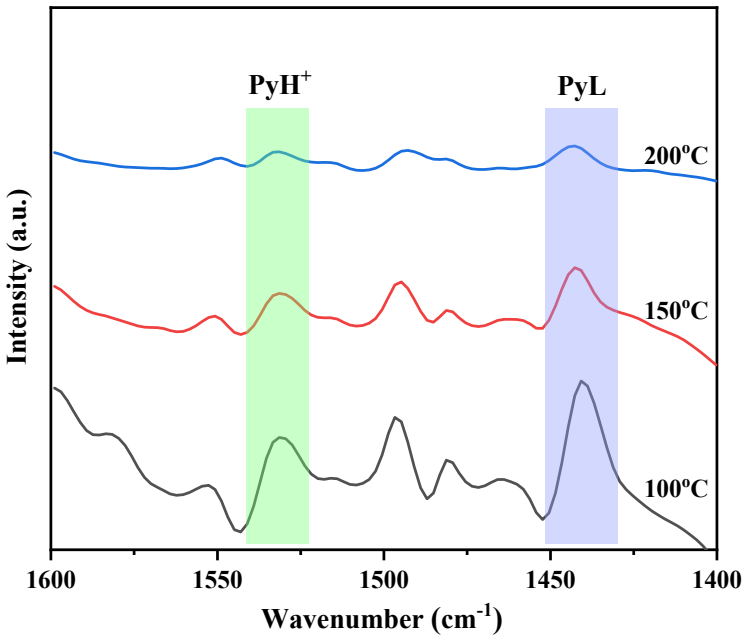

Figure S12. Pyridine-IR spectra of the $NbOPO_4$ sample.

Table S2. Investigation of acid sites of solid acids.

Catalyst	Additive	Acid sites (mmol g^{-1})	Conversion (%)	k (mL mg_{CoMoS}^{-1} h^{-1})
CoMoS	$NbOPO_4$	48.9	87.9	0.26
	H_4PMo_{12}	37.1	86.9	0.25
	H_4PW_{12}	20.7	86.0	0.24
	H_4SiW_{12}	19.0	85.3	0.24
	SiO_2	0	49.3	0.08

Discussion on the non-linear correlation between reaction rate constant and BA sites

The additional BA sites play an important role in the HDO reaction, but are not the only factor that influences the activity. As claimed in the main text, there is synergy effect between CoMoS and $NbOPO_4$. The two active phases can promote each other and both limit the activity at the same time. In detail, the BA and LA sites can help to adsorb p-cresol and accelerate the breaking of the C-O bonds. Then, the active H* dissociated by the Co-Mo-S phase can be provided for the hydrogenation step. Therefore, the active sites of the composite catalyst are abundant, and play their roles in common. Besides, the H_2 dissociated by CoMoS will further facilitate the generation of BA sites on $NbOPO_4$, so the amount of BA sites may change at the time. Actually, our pyridine-IR (Fig. 3) has confirmed a strong synergy between $NbOPO_4$ and CoMoS for increasing the total amounts of BA sites under hydrogen treatment condition. Generally, the number of BA sites cannot simply be thought of as linear relationships with the activity. As the acid sites increases, the limiting factor may be the BA sies at first and changed to another one after that. Therefore, the rate may not be in closer proportionality to the number of BA sites.

References

[1] Y. Zhang, J. Wang, J. Ren, X. Liu, X. Li, Y. Xia, G. Lu, Y. Wang, *Catal. Sci. Technol.*, 2012, 2, 2485-2491.

[2] H. Zhao, X. Hu, J. Hao, N. Li, K. Zhi, R. He, Y. Wang, H. Zhou, Q. Liu, *Appl. Catal. A,* 2020, 591, 117378.

[3] Q. Fang, Z. Jiang, K. Guo, X. Liu, Z. Li, G. Li, C. Hu, *Appl. Catal. B,* 2020, 263, 118325.

[4] J. Han, X. Ji, X. Ren, G. Cui, L. Li, F. Xie, H. Wang, B. Li, X. Sun, *J. Mater. Chem. A*, 2018, 6, 12974-12977.

[5] J. Kibsgaard, Z. Chen, B. N. Reinecke, T. F. Jaramillo, *Nat. Mater.*, 2012, 11, 963-969.

[6] Y. Zhang, T. Liu, Q. Xia, H. Jia, X. Hong, G. Liu, *J. Phys. Chem. Lett.,* 2021, 12, 5668-5674.

[7] V. N. Bui, D. Laurenti, P. Delichère, C. Geantet, *Appl. Catal. B*, 2011, 101, 246-255.

[8] J.V. Lauritsen, F. Besenbacher, *J. Catal.*, 2015, 328, 49-58.

[9] C. Kwak, J. J. Lee, J. S. Bae, K. Choi, S. H. Moon, *Appl. Catal.*, A 2000, 200, 233-242.

[10] K. Wu, W. Wang, H. Guo, Y. Yang, Y. Huang, W. Li, C. Li, *ACS Energy Lett.*, 2020, 5, 4, 1330-1336.

[11] G. Liu, A. W. Robertson, M. M. Li, W. C. H. Kuo, M. T. Darby, M. H. Muhieddine, Y. Lin, K. Suenaga, M. Stamatakis, J. H. Warner, S. C. E. Tsang, *Nat. Chem.*, 2017, 9, 810-816.

[12] W. Song, S. Zhou, S. Hu, W. Lai, Y. Lian, J. Wang, W. Yang, M. Wang, P. Wang, X. Jiang, *ACS Catal.,* 2019, 9, 259-268.